第 43 卷 第 15 期/2023 年 8 月/光学学报 特邀论文

光学学报

飞秒激光微加工蓝宝石晶片光纤压力传感器

江毅[1,2*]，张雨彤[1,2,3]，邓辉[1,2]

[1]北京理工大学光电学院，北京 100081；

[2]信息光子技术工业和信息化部重点实验室，北京 100081；

[3]包头师范学院物理科学与技术学院，内蒙古 包头 014030

摘要 提出了一种高温大量程的蓝宝石法布里-珀罗(F-P)干涉仪压力传感器。传感器由三层蓝宝石晶片直接键合而成，包括蓝宝石衬底、带通孔的蓝宝石晶片和感压蓝宝石晶片。飞秒激光用于在蓝宝石晶片的中心刻蚀通孔，并粗糙化感压蓝宝石晶片的外表面。利用蓝宝石晶片抛光面作为F-P腔的反射面，有助于降低解调出的光学腔长波动，提高压力分辨率。提出的传感器在室温、0～30 MPa的高压力范围内光学腔长随压力线性变化，压力灵敏度为0.1253 μm/MPa，相对分辨率达到0.04% FS(full scale，全量程)，且能在700 ℃下稳定工作。

关键词 光纤光学；光纤压力传感器；非本征法布里－珀罗干涉仪；蓝宝石晶片；飞秒激光微加工；大压力量程

中图分类号 TP212 **文献标志码** A **DOI:** 10.3788/AOS230732

1 引 言

随着航空航天、化工冶炼和石油电力等领域的发展，对高温恶劣环境中压力参数的实时在线监测有着广泛的需求[1-4]。传统的电学传感器已用于测量高温下的压力，例如压阻传感器[5-6]和电容传感器[7]。然而，受限于硅高温蠕变、高温漏电流增大及材料热膨胀系数不匹配等因素，电学传感器的工作温度一般低于600 ℃，并且存在电磁干扰和安全隐患等问题，使其无法应用于更高温度的恶劣环境中[8]。

光纤传感器以其无源、抗电磁干扰、耐高温、小巧等优点，能够应用于高温环境下各种参数的测量中，为恶劣环境下的测试测量提供了技术支撑[9-11]。光纤压力测量的最优技术途径是光纤非本征法布里-珀罗干涉仪(EFPI)，包括膜片式和无膜片式两种典型结构。无膜片光纤EFPI压力传感器的原理是开腔中的气体折射率随环境压力线性变化，因此该类传感器只能测量气体压力并且灵敏度受温度影响大[12-13]。基于不同材料的膜片式光纤EFPI压力传感器已广泛应用于压力测量领域[14-15]，传感器的工作温度主要由感压膜片的材料决定，如基于二氧化硅的EFPI压力传感器受限于高温下玻璃膜片的软化，一般长时间的工作温度低于800 ℃。针对超高温环境，需使用石英以外的基底材料，并且要求其在高温下有良好 的光学、热学和机械性能。

蓝宝石的主要成分为氧化铝(Al_2O_3)，熔点高达2045 ℃，具有高化学惰性、高强度、高硬度、高抗腐蚀性等特性，其光学透射窗口为0.5～3.5 μm，是一种研制高温压力传感器的理想材料[16]。近年的研究和应用表明，采用蓝宝石晶片微机电系统(MEMS)加工、蓝宝石键合技术制作EFPI腔，再用光纤对准获取干涉信号是具有工程应用价值的技术方案。Mills等[17]利用铂金属作为中间层对蓝宝石进行热压键合，在蓝宝石薄膜上镀钛和铂增强光的反射，传感器的工作温度达到了900 ℃。然而由于蓝宝石间含有中间层，蓝宝石腔在更高温度的密封性、稳定性上存在问题。Yi等[18]结合反应离子刻蚀工艺及蓝宝石直接键合工艺研制了用于压力测量的蓝宝石法布里-珀罗(F-P)腔，常温下在0.04～1.38 MPa的压力范围内对传感器进行了测试，之后Yi[19]用蓝宝石光纤获取干涉信号，25～1000 ℃范围内的压力响应结果表明，F-P腔密封良好，腔长随压力线性变化。邵志强等[20]对蓝宝石的湿法刻蚀工艺进行了研究，在280 ℃下，用体积比为1∶3的磷酸和硫酸混合溶液刻蚀蓝宝石晶片，凹槽表面的粗糙度达到0.39 nm，解调出的腔长波动降低至±5 nm。然而，干法、湿法刻蚀会增加蓝宝石晶片表面的粗糙度，导致信号解调精度下降，并且受限于传感器结构、键合强度等因素，目前研制的蓝宝石F-P腔压力量程限制在5 MPa内。

本文提出了一种飞秒激光微加工蓝宝石晶片光纤

收稿日期：2023-03-29；**修回日期**：2023-04-24；**录用日期**：2023-05-05；**网络首发日期**：2023-05-25

基金项目：国家自然科学基金(U20B2057)

通信作者：*bitjy@bit.edu.cn

压力传感器。传感头由直接键合的三片蓝宝石晶片构成，蓝宝石压力探头中间层通过飞秒激光刻蚀孔径不同的通孔，灵活控制传感器的灵敏度。依据膜片形变与施加压力呈线性关系，通过监测腔长变化来测量压力。搭建了超高压实验系统及高温压力实验系统，测试了传感器的压力响应和温度响应。实验结果表明，该传感器在45 MPa的高压下没有任何泄漏，可在高于700 ℃、0～30 MPa的压力范围内稳定工作。

2 传感器结构设计及工作原理

蓝宝石压力探头的结构示意图如图1所示。腔体采用三层结构，分别是蓝宝石衬底、带通孔的蓝宝石晶片及蓝宝石感压晶片。为使高压环境中蓝宝石衬底几乎不发生形变而感压膜片随压力线性形变，选取400 μm厚的蓝宝石晶片作为衬底，100 μm厚的蓝宝石晶片作为感压膜片。中间层采用175 μm厚的带通孔的蓝宝石晶片，较短的光程能够减少信号损耗。三层蓝宝石晶片通过直接键合固定。蓝宝石感压晶片外表面由飞秒激光粗糙化，蓝宝石衬底的两个抛光面作为测温F-P腔的两个反射面(R1和R2)，蓝宝石衬底和感压晶片的前抛光面作为测压F-P腔的两个反射面(R1和R3)，使用蓝宝石晶片原始的抛光面构成F-P腔，能够有效提升干涉信号的质量。图1中的三束反射光形成三光束干涉，干涉条纹可表示为

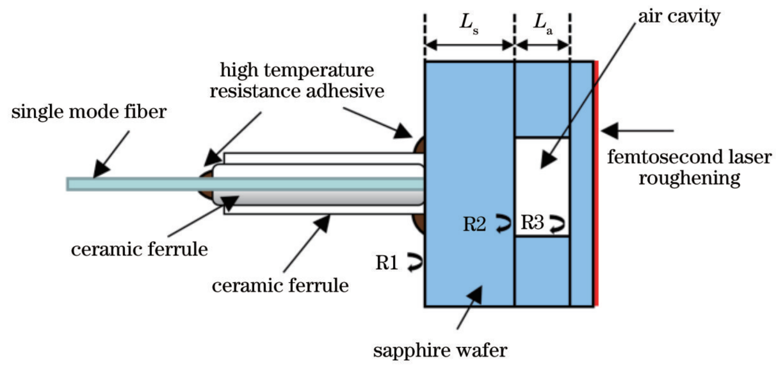

图1 传感头结构示意图

Fig. 1 Schematic diagram of sensor head

$$I = I_B + 2\gamma_1\sqrt{I_1 I_3}\cos\left[\frac{4\pi(n_s L_s + n_a L_a)}{\lambda}\right] - 2\gamma_2\sqrt{I_1 I_2}\cos\left(\frac{4\pi n_s L_s}{\lambda}\right) - 2\gamma_3\sqrt{I_2 I_3}\cos\left(\frac{4\pi n_a L_a}{\lambda}\right), \tag{1}$$

式中：I是三个反射面的总反射光强；I_B是背景光强；γ_1、γ_2、γ_3是三路双光束干涉信号的条纹对比度；n_s和n_a分别是蓝宝石和空气的折射率；L_s和L_a分别是蓝宝石衬底和空气腔的长度；λ为光波长。式(1)表明传感器的反射光谱由三个F-P腔干涉信号叠加组成，每路干涉信号是一个与光学腔长相关的余弦函数，均可以通过傅里叶变换白光干涉法实时解调[21-22]。

当外部压力作用在压力传感探头时，蓝宝石衬底厚度较大，几乎不发生形变，薄的感压膜片中心点形变可用挠度ω表示为

$$\omega = \frac{3r^4(1-\mu^2)}{16Eh^3}\cdot P, \tag{2}$$

式中：P是施加在感压膜片上的压强；E和μ分别是蓝宝石的杨氏模量和泊松比；h为感压膜片的厚度；r是通孔的半径。由式(2)得出蓝宝石感压膜片ω的形变与压强P正比，可以通过监测腔长的变化来测量压力的变化。由式(2)可知传感器的压力灵敏度为

$$S_P = \frac{d\omega}{dP} = \frac{3(1-\mu^2)r^4}{16Eh^3}。 \tag{3}$$

膜片的最大挠度小于其厚度的1/5时，认为其形变随压强是线性变化的，即

$$\Delta\omega = S_p\cdot\Delta P = \frac{3r^4(1-\mu^2)}{16Eh^3}\cdot\Delta P \leqslant 0.2h。 \tag{4}$$

式(3)和式(4)表明，增大通孔尺寸、减少感压膜片厚度能够提升传感器的灵敏度，但会降低压力传感器的线性工作范围，同时通孔尺寸的增大会导致键合强度降低，在超高压强下密封空气腔可能会泄漏。为实现在0～30 MPa的范围内保持高线性度且在45 MPa过载下密封腔不泄漏，本文传感器结构参数设为：r=0.625 mm，h=100 μm，蓝宝石的杨氏模量为380 GPa，泊松比为0.27，经计算，理论压力灵敏度为0.07 μm/MPa。

3 传感器制作

传感器的制作主要分为三个步骤：1)飞秒激光微加工蓝宝石晶片；2)蓝宝石晶片直接键合；3)传感器封装。

飞秒激光具有热损伤小、热影响区域小、加工精度高等特性，使用飞秒激光刻蚀蓝宝石晶片能够保证边缘的平整性，有效提高直接键合的成功率，本文使用的飞秒激光器为Spectra Physics的钛蓝宝石再生放大器Spitfire Ace，参数为800 nm的中心波长、35 fs的脉冲宽度和1 kHz的重复频率。首先，使用飞秒激光划片

将蓝宝石晶圆固定在六维微动平台，通过衰减片将激光功率调整至 30 mW，激光束通过焦距 100 mm 的平凸透镜垂直聚焦于蓝宝石晶圆表面，通过控制六维微动平台使激光在蓝宝石晶圆上以 5 mm 的间隔刻线。其次，在 175 μm 厚的蓝宝石晶片上刻蚀通孔。为了防止激光能量过大导致晶片碎裂，刻蚀内部通孔时将激光功率调整至 5 mW，用 20 倍物镜聚焦激光束，在蓝宝石晶片中心环形扫描至内部圆片自动脱落。最后，粗糙化感压蓝宝石膜片外表面。为了粗糙化膜片的同时尽量不改变膜片厚度，将激光功率调整至 1 mW，逐线扫描 100 μm 厚的蓝宝石晶片，划线间距为 50 μm。刻线的蓝宝石晶圆、切割好的蓝宝石衬底、带有通孔的蓝宝石晶片及粗糙化的感压膜片如图 2(a)所示。切割边缘的显微图如图 2(b)所示，能够看出其边缘平整，可用来键合。

为了提升传感器在高温、高压时的稳定性，本文设计了三层蓝宝石晶片的直接键合工艺。首先，对待键合的蓝宝石晶片进行 RCA 清洗，将蓝宝石晶片置于 120 ℃的食人鱼溶液[H_2SO_4(质量分数为 98%)∶H_2O_2(质量分数为 30%)=3∶1]中浸泡 15 min，用去离子水冲洗后，将晶片取出置于 80 ℃的 RCA-1 清洗液[NH_4OH(质量分数为 30%)∶H_2O_2(质量分数为 30%)∶H_2O=1∶2∶7]中浸泡 30 min，去离子水冲洗后浸泡在质量分数为 85% 的 H_3PO_4 中，升温至 150 ℃保持 30 min，去除表面残留的氧化物，清洗后的晶片放入稀 H_2SO_4 中沉积亲水性 OH^- 层。随后，蓝宝石晶片按照传感器三层结构对齐叠放，将四组晶片对放入陶瓷模具中。最后，模具上方放置 4 kg 的质量块，放入高温炉中，在 1300 ℃下保持 20 h，晶片界面间形成基于原子扩散的强键合，键合好的蓝宝石压力探头如图 3(a)所示。

采用单模光纤拾取蓝宝石压力探头的干涉信号。将去掉涂覆层的单模光纤插入到陶瓷插芯中，用耐高温胶固定，使用研磨机磨平光纤端面后插入陶瓷套管中，封装好的压力传感器如图 3(b)所示。

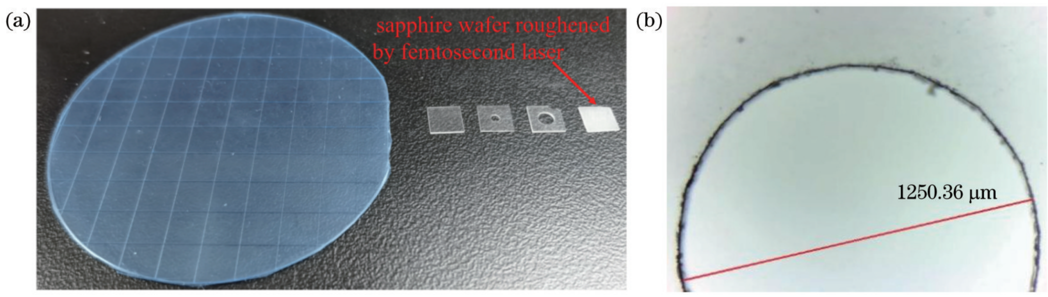

图 2 传感器制作。(a)飞秒激光加工的蓝宝石晶片；(b)切割边缘显微图

Fig. 2 Sensor fabrication. (a) Sapphire wafer processed by femtosecond laser; (b) micrograph of cutting edge

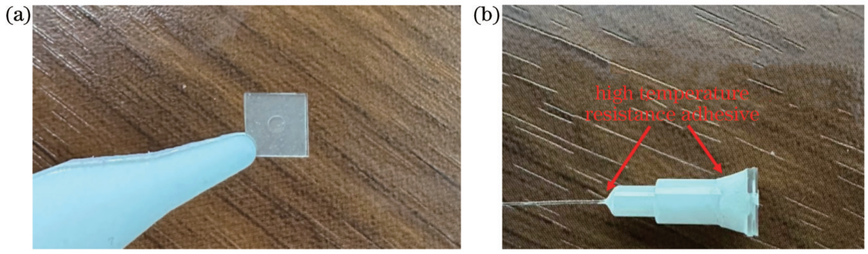

图 3 键合的传感器。(a) 蓝宝石压力探头；(b) 传感器封装

Fig. 3 Bonded sensor. (a) Sapphire pressure probe; (b) sensor package

4 实验结果及讨论

将传感器连接至实验室自制的光纤白光干涉解调仪[21]，其波长扫描范围为 1520～1570 nm，波长分辨率为 1 pm，采集到的光谱如图 4(a)所示，其频谱图如图 4(b)所示，能够看出反射光谱是由三光束干涉形成的，结合图 1 可知，第一个峰值为蓝宝石衬底后表面(R2)与感压膜片前表面(R3)形成的 F-P 信号，第二个峰值为蓝宝石衬底两个反射面(R1、R2)形成的 F-P 信号，第三个峰值为蓝宝石衬底前表面与感压膜片前表面(R1、R3)形成的 F-P 信号。图 4(b)表明，R2、R3 构成的 F-P 腔所形成的干涉信号较弱，因此，本文选用由 R1、R3 构成的 F-P 腔作为待测压力腔，R1、R3 构成的 F-P 腔作为待测温度腔。利用中心频率在主频位置的高斯窗函数提取主频信号，分别进行傅里叶逆变换，得到两个腔的干涉信号，如图 4(c)、4(d)所示。最后通过解调干涉信号的相位信息来计算光学腔长[22]。

超高压实验系统采用液压源产生高压，针对该压力测量系统，设计了传感器的封装。传感器装入不锈钢封装后，接到液压源的压力输出口，引出的光纤连接至解调仪，解调仪实时记录传感器待测压力腔的光学腔长。首先对传感器进行超高压老化。将适量水从进

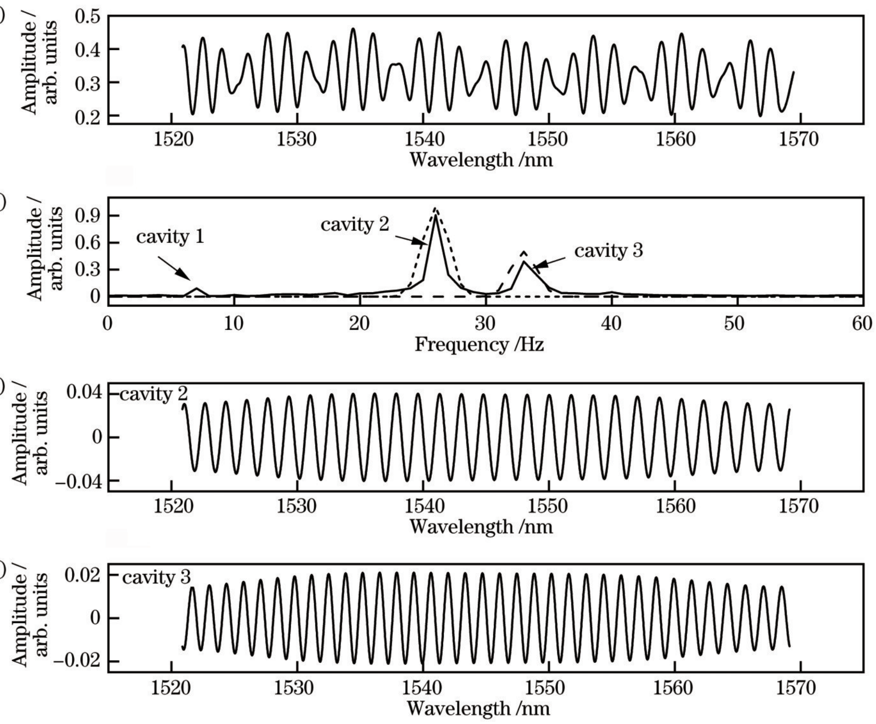

图4　信号解调过程。(a)传感器反射光谱；(b)频谱(实线)、高斯窗函数(短虚线、长虚线)；(c)傅里叶逆变换后的温度腔信号；(d)傅里叶逆变换后的压力腔信号

Fig. 4　Signal demodulation process. (a) Reflection spectrum of sensor; (b) frequency spectrum (solid line) and Gaussian windows (short dashed line and long dashed line); (c) temperature cavity signal after inverse Fourier transform; (d) pressure cavity signal after inverse Fourier transform

水口注入液压源，锁闭阀门，控制加压阀以1 MPa为间隔从0 MPa加压至30 MPa，记录传感器压力腔光学腔长变化，之后将压力升至45 MPa，保持1 h后降至0 MPa，经高压老化后的传感器再次进行0～30 MPa的压力实验，压力响应如图5所示。老化前传感器的压力灵敏度为0.0794 μm/MPa，与理论值0.07 μm/MPa十分接近。老化后传感器在0 MPa时的初始腔长发生了变化，且灵敏度变为了0.1253 μm/MPa，这可能是由于材料杨氏模量的变化所导致的。经多次压力测试，传感器初始腔长及压力灵敏度保持在老化后的状态，并在45 MPa时没有泄漏。

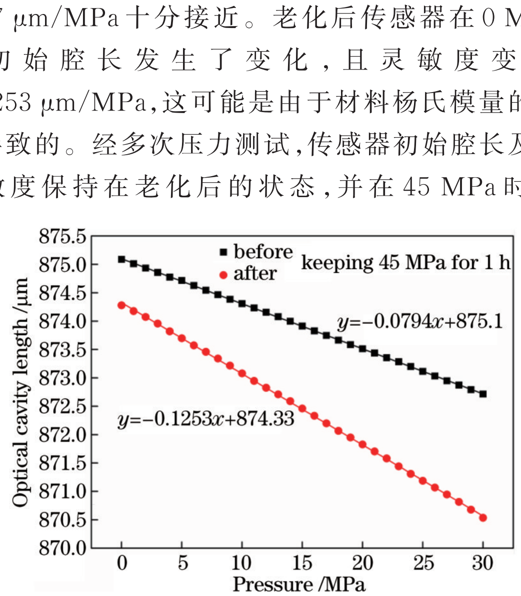

图5　0～30 MPa压力响应

Fig. 5　Pressure response of 0-30 MPa

为测试传感器在高温下的压力响应，搭建了如图6所示的测试系统。传感器放入陶瓷管中并置于马弗炉的恒温区，陶瓷管通过不锈钢管连接至压力罐，光纤从压力罐的光纤出口引出连接至解调仪。整套测试系统密封后，控制气压以1 MPa为间隔升压至5 MPa，在25～700 ℃范围内的压力响应如图7(a)所示，图中标注为对应温度点下的压力灵敏度。

图7表明，随着温度升高，传感器压力腔初始光学腔长增大，在每个温度点下，压力腔光学腔长随压力升高线性降低，证明传感器在高温下密封良好。由于温度升高材料杨氏模量下降，传感器压力灵敏度$S_P(T)$随着温度升高而略微增大，需监测环境温度去除温度对压力测量的影响。在测试传感器高温压力响应的同时，监测了传感器待测温度腔的光学腔长，温度响应如图8所示。

传感器在测量压力时，通过监测温度腔的光学腔长得到环境温度T，计算出该温度下的压力灵敏度$S_P(T)$，即得到环境压力为

$$P=\Delta L/S_P(T)+P_0,\qquad(5)$$

式中：ΔL是压力腔光学腔长变化；P_0是标准大气压。如当温度腔光学腔长为689 μm、压力腔光学腔长变化为0.4 μm时，由图8中拟合的压力响应可计算出环境温度为479 ℃，该温度下传感器的压力灵敏度为

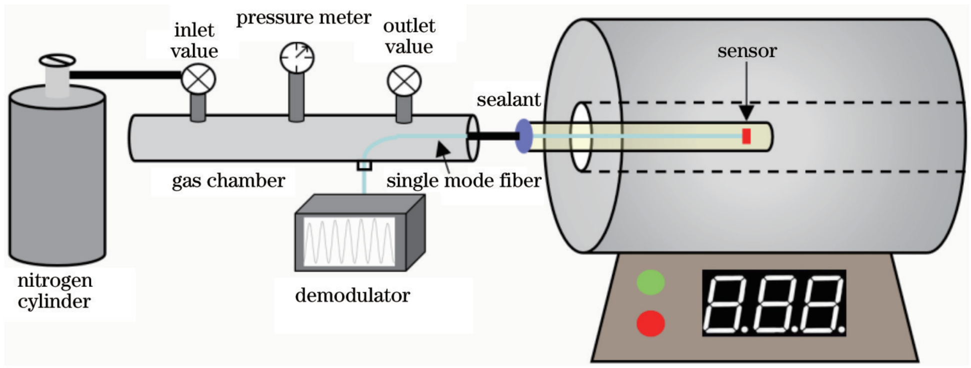

图 6　高温下压力响应测试系统

Fig. 6　Test system for pressure response at high temperature

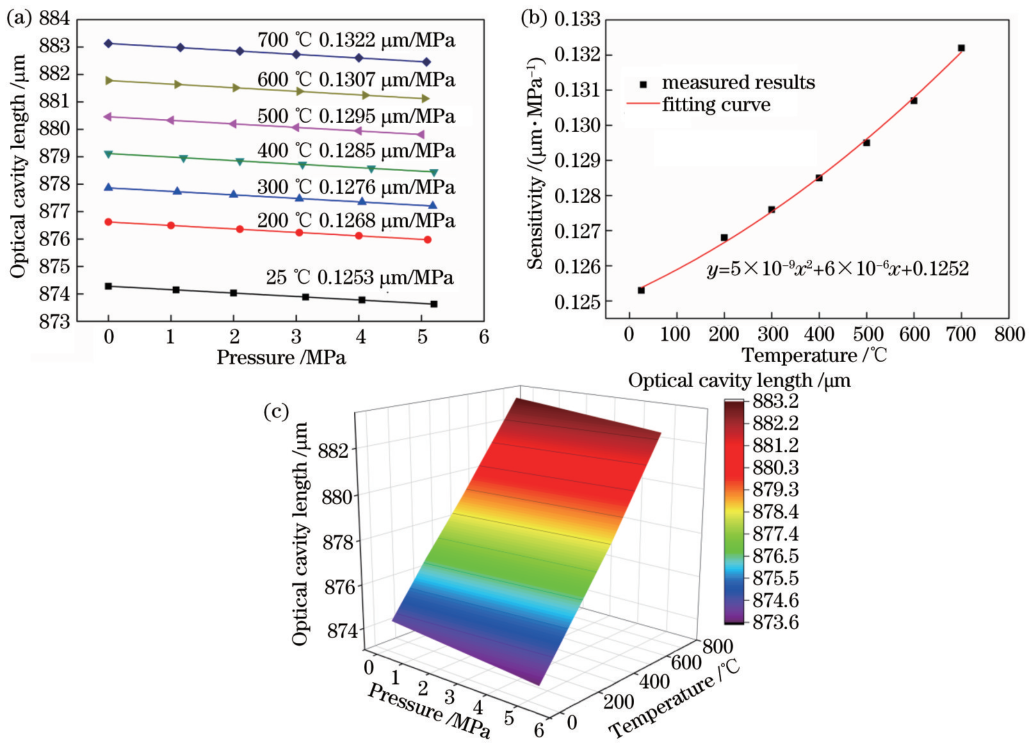

图 7　高温压力响应。(a) 25～700 ℃范围压力测试；(b)灵敏度随温度的变化；(c)腔长、温度、压力三维图

Fig. 7　Pressure response at high temperature. (a) Pressure test within range of 25-700 ℃; (b) sensitivity changes with temperature; (c) three-dimensional diagram of cavity length, temperature, and pressure

0.1292 μm/MPa，代入式(5)得此时的环境压力为 3.1 MPa。未来需用标准压力计对传感器进行标定。

最后，在室温和 10 MPa 的压力下，使用解调仪连续测量传感器压力腔的光学腔长。如图 9 所示，光学腔长的测量分辨率约为 1.5 nm，结合常温下传感器的压力灵敏度 0.1253 μm/MPa，超高压压力测量系统的压力分辨率为 12 kPa，相对分辨率为 0.04% FS(full scale，全量程)。

5　结　　论

本文提出了一种飞秒激光微纳加工蓝宝石晶片光纤压力传感器。蓝宝石晶片经飞秒激光加工成带通孔的晶片及粗糙化的感压膜片，通过直接键合形成密闭的 F-P 腔。实验结果表明，该传感器能够在 25～700 ℃、0～30 MPa 的高压力范围内测量压力，且传感器结构强度、键合强度满足在 45 MPa 的超高压力下不

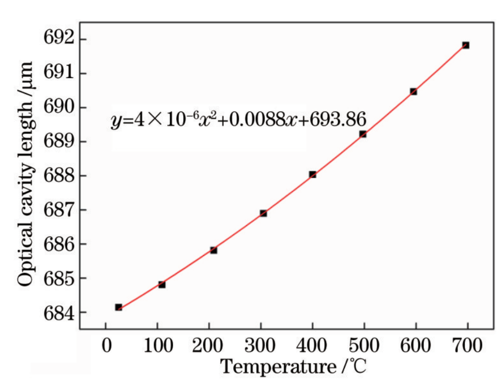

图 8　温度响应

Fig. 8　Temperature response

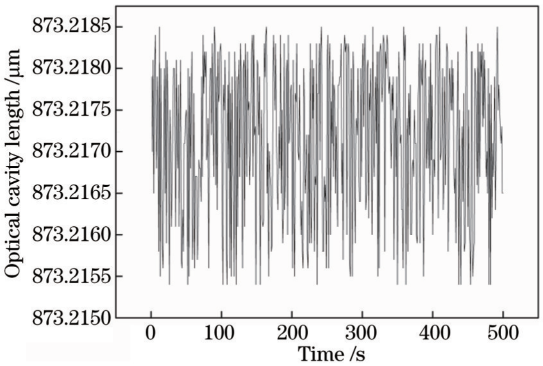

图9 10 MPa压力下光学腔长的波动

Fig. 9 Fluctuation of optical cavity length at 10 MPa pressure

碎裂、不泄漏。该传感器耐超高压、耐高温、本征安全、结构坚固,能够解决在高温高压恶劣环境下压力原位测试的技术难题。

参 考 文 献

[1] Javed Y, Mansoor M, Shah I A. A review of principles of MEMS pressure sensing with its aerospace applications[J]. Sensor Review, 2019, 39(5): 652-664.

[2] Yang J E. A harsh environment wireless pressure sensing solution utilizing high temperature electronics[J]. Sensors, 2013, 13(3): 2719-2734.

[3] 刘铁根, 王双, 江俊峰, 等. 航空航天光纤传感技术研究进展[J]. 仪器仪表学报, 2014, 35(8): 1681-1692.
Liu T G, Wang S, Jiang J F, et al. Advances in optical fiber sensing technology for aviation and aerospace application[J]. Chinese Journal of Scientific Instrument, 2014, 35(8): 1681-1692.

[4] 陈基亮, 孔德明, 郝虎, 等. 一种石油生产多分相检测新型光纤传感器[J]. 计量学报, 2022, 43(8): 1036-1043.
Chen J L, Kong D M, Hao H, et al. A new type of optical fiber sensor for multi-phase detection in petroleum production[J]. Acta Metrologica Sinica, 2022, 43(8): 1036-1043.

[5] Yao Z, Liang T, Jia P G, et al. A high-temperature piezoresistive pressure sensor with an integrated signal-conditioning circuit[J]. Sensors, 2016, 16(6): 913.

[6] Li C A, Cordovilla F, Jagdheesh R, et al. Design optimization and fabrication of a novel structural SOI piezoresistive pressure sensor with high accuracy[J]. Sensors, 2018, 18(2): 439.

[7] Li C, Sun B S, Jia P Y, et al. Capacitive pressure sensor with integrated signal-conversion circuit for high-temperature applications[J]. IEEE Access, 2020, 8: 212787-212793.

[8] Ren J A, Ward M, Kinnell P, et al. Plastic deformation of micromachined silicon diaphragms with a sealed cavity at high temperatures[J]. Sensors, 2016, 16(2): 204.

[9] Cui Y, Jiang Y, Liu T M, et al. A dual-cavity Fabry-Perot interferometric fiber-optic sensor for the simultaneous measurement of high-temperature and high-gas-pressure[J]. IEEE Access, 2020, 8: 80582-80587.

[10] 张硕, 江毅. 一种光纤高温压力传感器[J]. 仪表技术与传感器, 2018(1): 10-12, 70.
Zhang S, Jiang Y. Optical fiber high-temperature pressure sensor[J]. Instrument Technique and Sensor, 2018(1): 10-12, 70.

[11] 廖常锐, 何俊, 王义平. 飞秒激光制备光纤布拉格光栅高温传感器研究[J]. 光学学报, 2018, 38(3): 0308009.
Liao C R, He J, Wang Y P. Study on high temperature sensors based on fiber Bragg gratings fabricated by femtosecond laser[J]. Acta Optica Sinica, 2018, 38(3): 0308009.

[12] Zhang Z, He J, Dong Q, et al. Diaphragm-free gas-pressure sensor probe based on hollow-core photonic bandgap fiber[J]. Optics Letters, 2018, 43(13): 3017-3020.

[13] Xu B, Wang C, Wang D N, et al. Fiber-tip gas pressure sensor based on dual capillaries[J]. Optics Express, 2015, 23(18): 23484-23492.

[14] Ma W Y, Jiang Y, Gao H C. Miniature all-fiber extrinsic Fabry-Pérot interferometric sensor for high-pressure sensing under high-temperature conditions[J]. Measurement Science and Technology, 2019, 30(2): 025104.

[15] Jiang Y G, Li J A, Zhou Z W, et al. Fabrication of all-SiC fiber-optic pressure sensors for high-temperature applications[J]. Sensors, 2016, 16(10): 1660.

[16] Cui Y, Jiang Y, Zhang Y T, et al. Sapphire optical fiber high-temperature vibration sensor[J]. Optics Express, 2022, 30(2): 1056-1065.

[17] Mills D A, Alexander D, Subhash G, et al. Development of a sapphire optical pressure sensor for high-temperature applications[J]. Proceedings of SPIE, 2014, 9113: 91130H.

[18] Yi J, Lally E, Wang A B, et al. Demonstration of an all-sapphire Fabry-Pérot cavity for pressure sensing[J]. IEEE Photonics Technology Letters, 2011, 23(1): 9-11.

[19] Yi J. Sapphire Fabry-Pérot pressure sensor at high temperature[J]. IEEE Sensors Journal, 2021, 21(2): 1596-1602.

[20] Shao Z Q, Wu Y L, Wang S, et al. All-sapphire-based fiber-optic pressure sensor for high-temperature applications based on wet etching[J]. Optics Express, 2021, 29(3): 4139-4146.

[21] Jiang Y. High-resolution interrogation technique for fiber optic extrinsic Fabry-Perot interferometric sensors by the peak-to-peak method[J]. Applied Optics, 2008, 47(7): 925-932.

[22] Jiang Y. Fourier transform white-light interferometry for the measurement of fiber-optic extrinsic Fabry-Pérot interferometric sensors[J]. IEEE Photonics Technology Letters, 2008, 20(2): 75-77.

Optical Fiber Pressure Sensor Based on Sapphire Wafers Processed by Femtosecond Laser

Jiang Yi[1,2*], Zhang Yutong[1,2,3], Deng Hui[1,2]

[1]*School of Optics and Photonics, Beijing Institute of Technology, Beijing* 100081, *China*;

[2]*Key Laboratory of Photonic Information Technology, Ministry of Industry and Information Technology, Beijing* 100081, *China*;

[3]*School of Physical Science and Technology, Baotou Teachers´ College, Baotou* 014030, *Inner Mongolia, China*

Abstract

Objective Pressure monitoring in high-temperature environments is necessary for aerospace, chemical smelting, and petroleum power. Optical fiber sensors can be applied in the measurement of various parameters under high-temperature and harsh environment due to their advantages of passivity, anti-electromagnetic interference, high-temperature resistance, and compactness. The optimal technical approach for pressure measurement is the optical fiber extrinsic Fabry-Pérot interferometer (EFPI), which includes two typical structures of diaphragm-based type and diaphragm-free type. The principle of the diaphragm-free type is that as the refractive index of the gas in the open cavity changes linearly with the ambient pressure, diaphragm-free optical fiber pressure sensors can only measure the gas pressure, and its sensitivity is greatly affected by temperature. The diaphragm-type optical fiber EFPI pressure sensor based on different materials has been widely employed in pressure measurement. The working temperature of the sensor is mainly determined by the material of pressure sensing films. For example, the EFPI pressure sensor based on silicon dioxide is limited by the softening of the glass diaphragm at high temperature, and the working temperature for a long time is generally lower than 800 ℃. With a melting point of 2045 ℃ and a wide transmission spectral range, sapphire is an ideal material for developing ultra-high temperature optical fiber sensors. To measure pressure in high-temperature and harsh environment, we propose and experimentally demonstrate a sapphire Fabry-Pérot (F-P) interferometer with high temperature and large pressure range. The sensor is fabricated by direct bonding of three-layer sapphire wafers, including the sapphire substrate, the sapphire wafer with a through hole, and pressure-sensitive sapphire wafer.

Methods Firstly, a femtosecond laser is adopted to slice the sapphire wafer. The sapphire wafer is fixed on the six-dimensional micro-motion platform, and the laser power is adjusted to 30 mW through the attenuator. The laser beam is vertically focused on the surface of the sapphire wafer through a plano-convex lens with a focal length of 100 mm. The laser is scanned on the sapphire wafer at 5 mm intervals by controlling the six-dimensional micro-motion platform. Secondly, a through hole is inscribed on a sapphire wafer with a thickness of 175 μm. The laser power is adjusted to 5 mW, and the laser beam is focused by a 20× objective lens. The laser scans in the center of the sapphire wafer until the inner wafer falls off automatically. Thirdly, the outer surface of the sapphire diaphragm is roughened. The laser power is adjusted to 1 mW to roughen the diaphragm without changing the thickness of the diaphragm as much as possible. The laser scans the surface by line-by-line method with a spacing of 50 μm. Finally, to improve the stability of the sensor at high temperature and high pressure, the direct bonding process of sapphire wafers is designed. After RCA cleaning, sapphire wafers are immersed in 85% (mass fraction) H_3PO_4 solution to remove residual oxides on the surface. Then wafers are immersed in a H_2SO_4 diluted solution to deposit a hydrophilic layer. The wafer pair is successfully bonded after being kept at 1300 ℃ for 20 h and pressure test systems are set up to investigate the pressure response of the proposed sensor.

Results and Discussions The EFPI interference signal collected by the white light interference demodulator with a center wavelength of 1550 nm is shown in Fig. 4(a), and its frequency spectrum is shown in Fig. 4(b). The reflection spectrum is formed by three-beam interference. The second peak is the F-P signal formed by two surfaces (R1, R2) of the sapphire substrate, which is utilized to measure the temperature. The third peak is the F-P signal formed by the front surface of the sapphire substrate and the front surface of the pressure-sensing sapphire diaphragm (R1, R3), which is leveraged to measure the pressure. The main frequency signal is extracted by the Gaussian window function, and the interference signals of the two cavities are obtained by inverse Fourier transform. The optical cavity length can be calculated by demodulating the phase information of the interference signal. The ultra-high pressure test shows that the pressure sensitivity of the sensor is 0. 1253 μm/MPa within the pressure range of 0–30 MPa, and the sensor has no leakage at 45 MPa. As the temperature increases, the sensitivity of the sensor increases slightly, reaching 0. 1322 μm/MPa at 700 ℃. Figure 9 shows that the measurement resolution of the optical cavity length is about 1. 5 nm. Combined with the pressure sensitivity of the sensor at room temperature, the pressure resolution of the ultra-high pressure measuring system is 12 kPa, and the relative resolution is 0.04% FS (full scale).

Conclusions In this study, an optical fiber pressure sensor based on sapphire wafers processed by femtosecond laser is proposed. Sapphire wafers with through holes and rough sapphire pressure-sensitive wafers are fabricated by femtosecond laser micromachining. The experimental results show that the sensor can measure the pressure within the temperature range of 25-700 ℃ and the wide pressure range of 0-30 MPa, and the sensor does not break and leak under the ultra-high pressure of 45 MPa. The sensor is resistant to ultra-high pressure, high temperature, and intrinsic safety, which can solve the technical problems of pressure *in-situ* testing in the harsh environment of high temperature and high pressure.

Key words fiber optics; optical fiber pressure sensors; extrinsic Fabry-Pérot interferometer; sapphire wafer; femtosecond laser micromachining; large pressure range